THESIS

A COMPARISON OF POSITIVE AND NEGATIVE CLOUD-TO-GROUND LIGHTNING DOMINANT STORMS IN THREE REGIONS OF THE UNITED STATES

Submitted by

Amanda R. S. Anderson

Department of Atmospheric Science

In partial fulfillment of the requirements

For the Degree of Master of Science

Colorado State University

Fort Collins, Colorado

Summer 2011

Master's Committee:

Advisor: Steven Rutledge

Timothy Lang
Sue van den Heever
R. Steve Robinson

ABSTRACT

A COMPARISON OF POSITIVE AND NEGATIVE CLOUD-TO-GROUND LIGHTNING DOMINANT STORMS IN THREE REGIONS OF THE UNITED STATES

A statistical framework for analyzing storm data, called CLEAR (Colorado State University Lightning, Environment, Aerosols, and Radar), was used to examine the characteristics of seven storms in three different regions of the contiguous United States. Regions included the High Plains (eastern Colorado/western Kansas), central Oklahoma, and northern Alabama. Dual-polarization radar, lightning mapping array observations, and environmental reanalysis data were ingested by CLEAR to objectively assign lightning and environmental information to tracked storms. Comparison of environmental characteristics of the positive cloud-to-ground lightning (+CG) and negative cloud-to-ground lightning (-CG) dominant storms in the three regions showed no clear environmental difference between storms of different CG polarity dominance or between the regions themselves. Analysis of the lightning data showed the layer of maximum Very High Frequency (VHF) source density, inferred to be the positive charge layer, of the +CG dominant storms was at a much lower height (warmer temperature) than that of the -CG dominant storms. This indicated the probable existence of an inverted charge structure in the +CG dominant storms and supports previous research that

suggested inverted charge as a cause of +CG dominance. Additionally, dual-Doppler analysis of the storms found that the +CG dominant storms had a much larger volume of >10 m s^{-1} updraft than the -CG dominant storms, which may contribute to the production of the inverted charge structure. The +CG dominant storms also had larger graupel echo volumes, consistent with the larger updraft volumes.

ACKNOWLEDGEMENTS

I would first like to thank my advisor, Dr. Steven Rutledge, for his support and guidance during this project as well as allowing me to pursue a full-time job when the opportunity arose before my work was completely finished. I also want to thank Dr. Timothy Lang for his support on this project, including scientific guidance and education on research methodologies. Also a thank you for the great support from my committee members Dr. Sue van den Heever and Dr. R. Steven Robinson.

Paul Hein provided essential computer support, and I highly appreciate his efforts. Dr. Rob Cifelli provided excellent advice during my work. I would also like to thank all members of the CSU Radar Group for their advice and for listening as I talked through my ideas, especially my officemates Angela Rowe and Brenda Dolan Cabell. Also a thank you to all my family and friends for their support in my research and education goals.

Finally, I would like to thank Dr. Terry Schuur and Dr. Don MacGorman of the National Severe Storms Laboratory for providing KOUN and Oklahoma LMA data, and Dr. Walter Petersen of NASA MSFC and Elise Johnson of the University of Alabama in Huntsville for providing ARMOR and Alabama LMA data. NLDN data were obtained from Vaisala. This research was supported by grants from the National Science Foundation (ATM-0649034 and AGS-1010G6S7).

TABLE OF CONTENTS

LIST OF TABLES

LIST OF FIGURES

CHAPTER 1

Introduction

Past studies of cloud-to-ground (CG) flash distributions have shown that the density of positive CG (+CG) flashes, compared to the density of negative CG (-CG) flashes, varies throughout different regions of the United States (e.g., Orville 2002). Specifically, the High Plains region of the United States experiences a higher percentage of +CG flashes than other areas of the country, particularly the Gulf Coast region.

Such regional variability of the electrical structure of storms has been the subject of many studies (e.g., Lyons et al. 1998; Smith et al. 2000; Zajac and Rutledge 2001; Carey et al. 2003), and overall these studies have found that storms with a high percentage of +CG flashes tended to occur in environments more conducive of strong convection, i.e. larger instability and wind shear, as well as somewhat drier environments that lead to smaller warm-cloud depths, such as the High Plains.

Some of the difficulty in comparing storms across different regions lies in the use of different data sources in the different areas, such as different radars. To overcome this challenge, the Colorado State University (CSU) Lightning, Environment, Aerosols, and Radar (CLEAR) framework was used for this study (Lang and Rutledge 2011). CLEAR is capable of ingesting a large variety of data sources and types and combining them into standardized files, which allows the comparison of both large volumes of data as well as data from a variety of different sources, such as would be needed to compare storms among different regions.

This study performs a first step in addressing questions of regional differences in lightning structure by using CLEAR to examine seven storms in three climatologically different regions of the United States: the western High Plains, central Oklahoma, and northern Alabama. These three regions were chosen based on the availability of both dual polarization Doppler radar and a lightning mapping array, which allowed for the study of the microphysical and total lightning characteristics of the storms. The CLEAR framework was used to merge radar, lightning, and environmental data from the three regions into a similar format that allowed efficient comparisons between the storms. The way in which regional differences between storm environments may contribute to differences in the electrical structure of the storms was examined, particularly in relation to +CG and -CG dominance.

This thesis is organized into five chapters. Chapter 2 provides background on thunderstorm charging, environmental variability in relation to inverted charge structures, and the CLEAR framework. Chapter 3 presents the data and methodology used for the analysis. Chapter 4 gives a brief overview of the seven cases, Chapter 5 presents the results of the analysis, and Chapter 6 gives conclusions and future work.

CHAPTER 2

Background

2.1 Thunderstorm charging and charge structure

The non-inductive charging (i.e., charging outside of a preexisting electric field) of graupel and ice particles in the presence of supercooled liquid water has emerged as the most plausible mechanism for electrifying clouds as collaborated by detailed laboratory and modeling studies (MacGorman and Rust 1998). In this hypothesis, graupel grows by riming in the presence of supercooled liquid water and collides with smaller ice crystals, resulting in charge transfer where the graupel and ice particles will be of opposite charge. Gravitational settling then separates the graupel particles, which fall to lower levels, from the lighter ice crystals, which are lofted to or remain in higher levels. Additional charging hypotheses can be found in MacGorman and Rust (1998).

The specific environments that lead to the polarity of the charged graupel and ice crystals have been examined in laboratory experiments, including Takahashi (1978) and Saunders and Peck (1998). Results of the Takahashi (1978) study are summarized in Figure 2.1. The sign of the charge on the riming particle (i.e., graupel) was dependent on the air temperature and cloud water content of the particle's environment. Generally, particles at -10 °C or warmer acquired a positive charge regardless of the cloud water content. Below -10 °C, relatively high or low cloud water contents (approximately

< 0.25 to > 4 g m^{-3} though this varies with temperature) tended to result in positive charging, with intermediate water contents resulting in negative charging.

The charge structure of thunderstorms is typically arranged in the form of a tripole, where a large negative charge region forms in the mid levels of the storm with a large positive charge region above, along with another, usually small, positive charge region below the negative (William 1989, 2001). A conceptual model of this charge structure can be found in Fig. 2.2. Relating this back to the inductive charging mechanism, negatively charged graupel particles would tend to settle in mid levels where the normal tripole's negative charge layer is found, and the positively-charged ice crystals would settle in the upper levels. This settling is a result of the balance between gravitational forces and the force of the storm's updraft. The smaller positive charge layer at the bottom of the storm may be due to inductive charging in the presence of the electric field generated by the higher-level charge layers (MacGorman and Rust 1998).

Several studies have linked storms producing predominately +CG lightning to inverted charge structures (e.g., Rust and MacGorman 2002; Lang et al. 2004; Rust et al. 2005; Wiens et al. 2005; Tessendorf et al. 2007; to name a few). Additional hypotheses have been advanced for the production of predominately +CG lightning, and the reader is directed to Williams (2001) for a discussion of these. For the inverted charge structure specifically, graupel, which would take on a negative charge in the normal charge structure scenario, takes on a positive charge in collisions with ice crystals, possibly due to elevated levels of liquid water as presented by Takahashi (1978). Rebounding ice crystals acquire net negative charge. Gravitational settling results in a large positive charge region in the mid levels and a large negative charge region above it, opposite the charge structure in Fig. 2.2.

2.2 Regional environment variability and formation of inverted charge structure

Regional variability of the electrical structure of storms has been the subject of many studies. Lyons et al. (1998) examined large peak current (≥ 75 kA) CG flashes across the United States, finding that large current +CG flashes were concentrated over the High Plains and upper Midwest while large peak current -CG flashes were concentrated over the southeastern United States. Zajac and Rutledge (2001) studied CG lightning across the contiguous United States and found that, overall, a larger percentage of -CG lightning was produced during the summer, and the diurnal cycle of +CG lightning lagged that of -CG lightning by up to two hours during the summer. The exception to this was in the north-central United States, where +CG lightning occurrence peaked during the midsummer versus late summer for -CG lightning, and the diurnal cycle peak of +CG lightning preceded the peak of the diurnal cycle of -CG lightning by several hours.

Regional differences in the prevalence of +CG lightning naturally lead to the question of why +CG lightning tends to occur more frequently, or as a larger percentage of total CG lightning, in specific regions of the United States. A study of the climatology of CG lightning polarity in severe storms across the contiguous United States by Carey et al. (2003) found that 61% of severe storms had > 90% -CG lightning, but 43% of severe storms in the northern plains had > 50% +CG lightning. These climatology findings were in line with the results of Smith et al. (2000), which found that the majority of -CG dominant storms formed in regions of weak equivalent potential temperature gradient (θ_e) and downstream of a θ_e maximum, while +CG dominant storms formed in an area of strong surface θ_e gradients and often upstream of a θ_e maximum. In the Carey et al. (2003) study, the +CG dominant severe storms generally occurred west and northwest of the θ_e ridge in a θ_e gradient or within the θ_e ridge in regions under the influence of polar fronts during the warm season. Carey and Buffalo (2007) examined the hypothesis that the inverted charge structures that promote +CG lightning production seem to be associated with broad, strong storm-scale updrafts and large liquid water contents that result from them. The particular environment that favors such updrafts should then support the formation of inverted polarity storms. They found that +CG dominant storms were associated with a drier low-level to mid-level troposphere, higher cloud-base height, smaller warm-cloud depth, stronger conditional instability, larger 0-3 km wind shear, and larger convective available potential energy (CAPE). These parameters relate to the production of +CG flashes by their role in producing strong, broader updrafts and higher liquid water contents in the mixed-phase zone.

2.3 The Colorado State University analysis framework

To help address the issue of ingesting and analyzing large radar, lightning, environmental, and aerosol datasets from a variety of instruments, as would be necessary for regional comparisons of lightning characteristics, the Colorado State University (CSU) Lightning, Environment, Aerosols, and Radar (CLEAR) framework was developed at CSU (Lang and Rutledge, 2011). As presented in the Lang and Rutledge study, CLEAR is capable of ingesting a large variety of data sources and types and combining them into standardized files, which allows the comparison of both large volumes of data as well as data from a variety of different sources, such as would be needed to compare storms among different regions. In their analysis, Lang and Rutledge (2011) performed a statistical analysis of cases from the Severe Thunderstorm Electrification and Precipitation Study (STEPS; Lang et al. 2004), focusing on the differences between +CG dominant and -CG dominant storms. They found that +CG dominant storms were overall more electrically active as marked by Very High Frequency (VHF) radio-frequency source density and contained mid-level positive charge compared to -CG storms, which tended to be less electrically active and contained mid-level negative charge. Additionally, storms that were +CG dominant were of larger radar echo volume and were more vertically developed compared to their -CG-dominated counterparts. The +CG dominant storms were also associated with environments supportive of intense convection, i.e. increased moisture, wind shear, and instability.

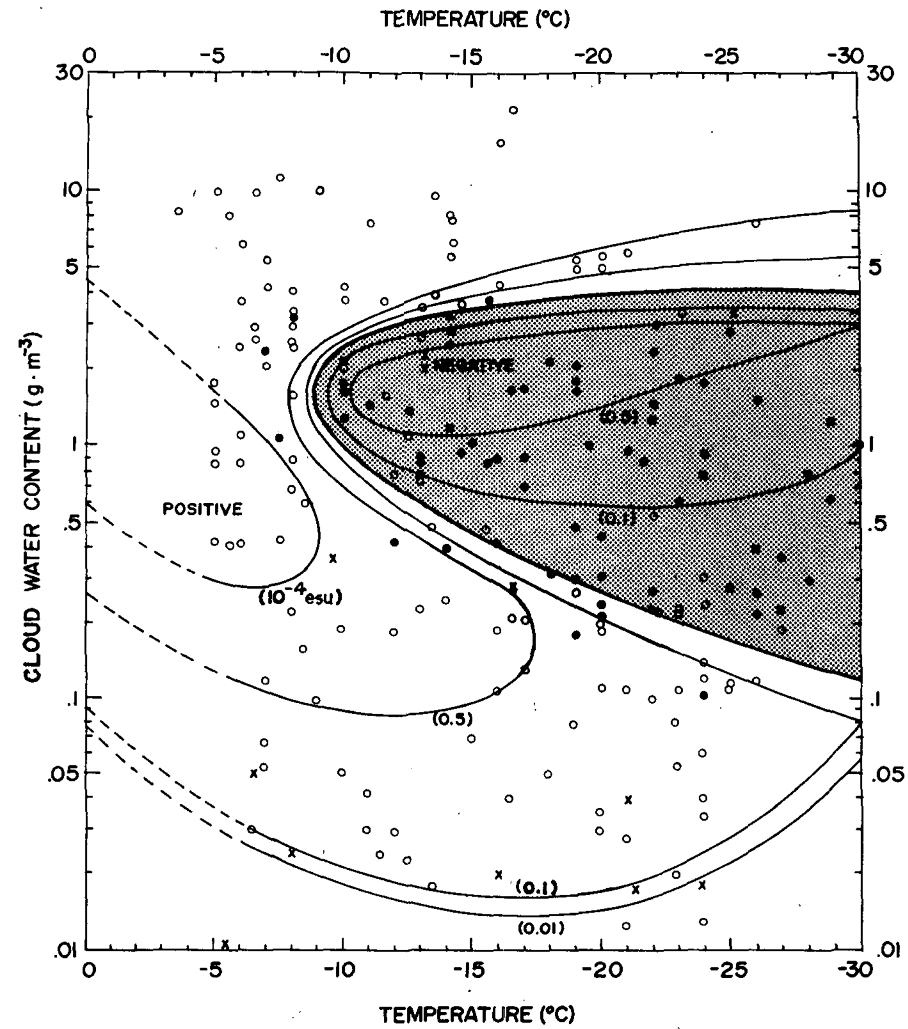

Fig. 2.1: Charging of riming of particles by air temperature and cloud water content. Positively charged particles are shown as open circles, negatively charged particles as solid circles, and uncharged cases as X's. The general negative charging area is shaded, the positive charging area is white. From Takahashi (1978).

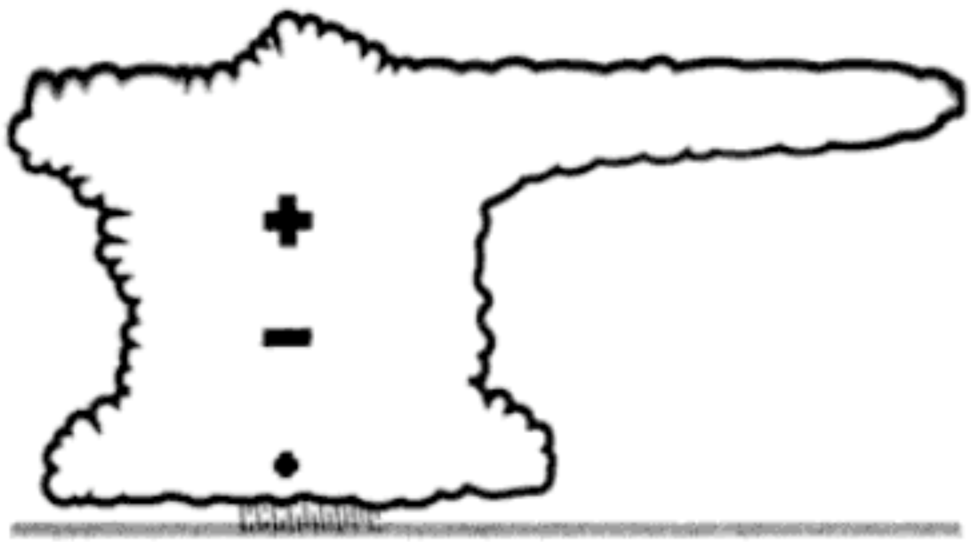

Fig. 2.2: A conceptual schematic of thunderstorm charge structure for a normal tripole. From MacGorman and Rust (1998).

CHAPTER 3

Data and Methods

The three regions used in this study were chosen based on the availability of both dual-polarization radar data and an LMA network in order to examine both the microphysical and the total lightning characteristics of the storms. Two to three storms were subjectively chosen from each region with the criteria that they be isolated and produce severe winds, severe hail, and/or tornadoes. The definition of severe here is that used by the National Weather Service (NWS) as recorded by Storm Prediction Center (SPC) severe weather reports. Radar images from the operational NWS WSR-88D radars were downloaded from the National Climate Data Center (NCDC) and were examined to determine if the storms were isolated. This was done by converting the NWS formats to sweep files, which could be viewed through the National Center for Atmospheric Research (NCAR) SOLOii program (Oye et al. 1995). SPC storm reports (Storm Prediction Center 2008) were visually matched with the storms to determine their severity. This was done by looping through radar images of each storm and comparing the storm location with the SPC storm reports to determine if the prospective storms were associated with severe weather conditions.

3.1 Radar data and analysis

Polarimetric radar data were obtained from the following radars: the Colorado State University-CHILL (CSU-CHILL; Brunkow et al. 2000) and the NCAR S-Pol (Keeler et al. 2000) radars in the High Plains, the University of Oklahoma's KOUN radar (Ryzhkov et al. 2005) in central Oklahoma, and the University of Alabama Huntsville-National Space Science and Technology Center (NSSTC) Advanced Radar for Meteorological and Operational Research (ARMOR; Petersen et al. 2009) in northern Alabama. Data from CSU-CHILL/S-Pol were collected during STEPS (Lang et al. 2004), and both radars were S-band using alternating transmit and receive and collected a full suite of polarimetric variables. A setup of the STEPS network with locations of CHILL and S-Pol can be found in Fig. 3.1. KOUN data were collected during the Thunderstorm Electrification and Lightning Experiment (TELEX; MacGorman et al. 2008). KOUN is also an S-band radar, but operates in a simultaneous transmit and receive configuration. A setup of the TELEX network is given in Fig. 3.2. ARMOR data were collected independent of a field program. This radar is a C-band radar that operates with simultaneous transmission of horizontal and vertical polarization. A setup of the test bed around ARMOR is given in Fig. 3.3.

The reflectivity data from the High Plains and central Oklahoma S-band radars were corrected for gaseous attenuation by adding a factor of 0.014 multiplied by the range of the bin. Data were then filtered based on a co-polar correlation coefficient (ρ_{HV}) threshold of 0.6 and a standard deviation of the differential propagation phase (ϕ_{DP}) threshold of 18° within an Interactive Data Language (IDL) procedure. Additionally, ϕ_{DP} itself was filtered using a 21-point finite impulse response (FIR) filter as described by

Hubbert and Bringi (1995), which separated the differential propagation phase from the backscatter propagation phase in ϕ_{DP}, allowing a more accurate specific differential phase (K_{DP}) calculation. The K_{DP} was calculated based on the filtered ϕ_{DP} using a finite-difference approximation, also performed with an IDL procedure. Remaining clutter and spurious echo was removed manually using the NCAR SOLOii program (Oye et al. 1995) by the "despeckle" feature.

After this processing, the radar data were interpolated from radar space to Cartesian space using the NCAR REORDER software (Oye et al. 1995). The grids were centered at the KOUN radar for central Oklahoma storms. For High Plains storms, the grids were centered at the NWS Goodland, KS radar (KGLD) for consistency with past case studies of STEPS storms (e.g., Tessendorf et al. 2005; Wiens et al. 2005; Tessendorf et al. 2007). Grid spacing was 0.5 km. The ARMOR data were provided to the authors already filtered and gridded by the University of Alabama in Huntsville, centered on the ARMOR radar, at a grid spacing of 1.0 km.

For storms that occurred in a region where dual-Doppler techniques could be used to analyze the wind fields, the NCAR Custom Editing and Display of Reduced Information in Cartesian Space (CEDRIC; Mohr et al. 1986) software was used to globally unfold velocities, then again to calculate the three-dimensional wind field. In all cases, it was confirmed that the storm was topped by the radars, allowing a variational downward integration scheme to be used. Downward integration was preferred to upward for these cases because errors in the vertical velocity are dampened with an integration from lower to higher density, and the variational method distributes the error remaining at the boundaries, i.e. if $w \neq 0$ at the surface (Bohne and Srivastava 1975).

Finally, hydrometeor identification was performed using a fuzzy logic hydrometeor classification as in Tessendorf et al. (2005), which was adapted from Liu and Chandrasekar (2000) and Straka et al. (2000). This process uses dual-polarization radar parameters and a temperature profile to produce the most likely hydrometeor type based on the polarimetric observations for each grid point in the analysis domain. In this method, hydrometeors are calculated using a set of so-called beta functions corresponding to the input variables and resulting possible classifications. This results in several truth values, and the returned hydrometeor is that with the highest truth value for the grid point. It is important to note that the hydrometeor classification was developed for use with S-band radar systems, while the ARMOR radar operates at C-band. As presented by Marzano et al. (2006), Mie-scattering effects in C-band data are more sensitive to particle shapes and orientations compared to S-band data, and therefore a hydrometeor classification algorithm developed for S-band data results in misclassifications when applied to C-band data. For the study in this thesis, hydrometeor classifications of the C-band data were only examined in terms of graupel echo volume, and the S-band tuned classification is considered to provide a physically realistic estimate of graupel echo volume for the storms observed by ARMOR.

3.2 Lightning data and analysis

Lightning data were obtained from LMA networks in the three regions. The LMA is a Global Positioning System (GPS)-based network to map lightning flashes in three dimensions by detecting sources of VHF radiation produced by the lightning discharges (Rison et al. 1999). The National Lightning Detection Network (NLDN;

Cummins et al. 1998) data were used to identify CG flashes. The LMA network used during STEPS in the High Plains was the deployable LMA from the New Mexico Institute of Mining and Technology (NMIMT; Lang et al. 2004; Fig. 3.1). The LMA in central Oklahoma was acquired from NMIMT and is operated by the University of Oklahoma, the National Severe Storms Laboratory, and NMIMT (MacGorman et al. 2008; Fig. 3.2). The North Alabama 3-D VHF regional LMA contains ten receivers deployed across northern Alabama and was also acquired from NMIMT (Goodman et al. 2005; Fig. 3.3).

LMA analysis for all regions was performed in the same way. Data were thresholded on $\chi^2 \leq 1$ and the VHF point being detected by a minimum of seven LMA stations to reduce data noise. VHF sources that were outside of the storm area (i.e., VHF sources outside of the cluster of sources in the storm area) were removed from the analysis area prior to identifying flashes. This isolation is not necessary, but it was done to speed up the flash analysis process. In-cloud flashes were identified using the built in algorithm in the XLMA program, developed by NMIMT (Thomas et al. 2003). The XLMA program is written in the IDL language and serves as a method of viewing and processing the VHF source data from LMA networks (Fig. 3.4). The program window displays the time and location in three dimensions of VHF sources detected by the LMA. The built in algorithm uses time and space to determine which sources should be linked together as a flash. CG flashes detected by the NDLN were also processed by XLMA. The +CG flashes were thresholded at current > 10 kA following the recommendation of Cummins et al. (1998) to try to eliminate false detection of positively charged in-cloud flashes. Note that in the case of very high flash rates, such as those observed in the

29 May 2004 storm from TELEX, the magnitude of the flash rates are more highly influenced by small changes in thresholding, making the trends of the flash rate more important than the flash rate itself in these cases (MacGorman et al. 2008).

3.3 Environmental data and analysis

Environmental data were obtained from the Atmospheric Radiation Measurements (ARM) archive of the Rapid Update Cycle (RUC) analyses (Benjamin et al. 2004). The RUC data were chosen as opposed to observed soundings due to the lack of spatial and temporal resolution of operational soundings. These data were received on a 20-km grid and isobaric vertical levels. No additional analysis was performed on these data before their integration into CLEAR.

3.4 Statistical framework synthesis

A more thorough description of the statistical framework, CLEAR, can be found in Lang and Rutledge (2011). Figure 3.5 gives a schematic of the CLEAR framework. For the present study, storm cells were tracked using an in-house hybrid tracking algorithm, as described by Rowe et al. (2011). This algorithm identifies storm cells based on 35-dBZ and 45-dBZ contours (similar to the Storm Cell Identification and Tracking, SCIT, algorithm's use of multiple reflectivity levels; Johnson et al. 1998), then tracks the centroids using an ellipse drawn around the cell (similar to the Thunderstorm Identification, Tracking, Analysis, and Nowcasting, TITAN, algorithm; Dixon and Wiener 1993). Statistical framework modules were then used to objectively assign lightning flashes to the specific storm cells tracked as shown in Fig. 3.5. Specifically, the LMA data, consisting of individual VHF sources and counted flashes analyzed from XLMA, and the NLDN data, consisting of the flash and current, along with their location in space and time, were assigned to the tracked feature in which they were contained and added to the gridded radar Network Common Data Form (NetCDF) file. Finally, environmental data from the RUC analyses were assigned to the tracked storms. This was done by linearly interpolating the RUC data across two successive hourly analysis times to the radar volume time. Then, RUC analysis of storm motion was used to advect the feature location to the nearest grid point downstream. The storm motion was used to advect the storm feature location so the RUC data would be more representative of the storm inflow. The result was a NetCDF file for each radar volume containing identified storm cells with assigned lightning flashes and environmental parameters, with which the analysis was performed.

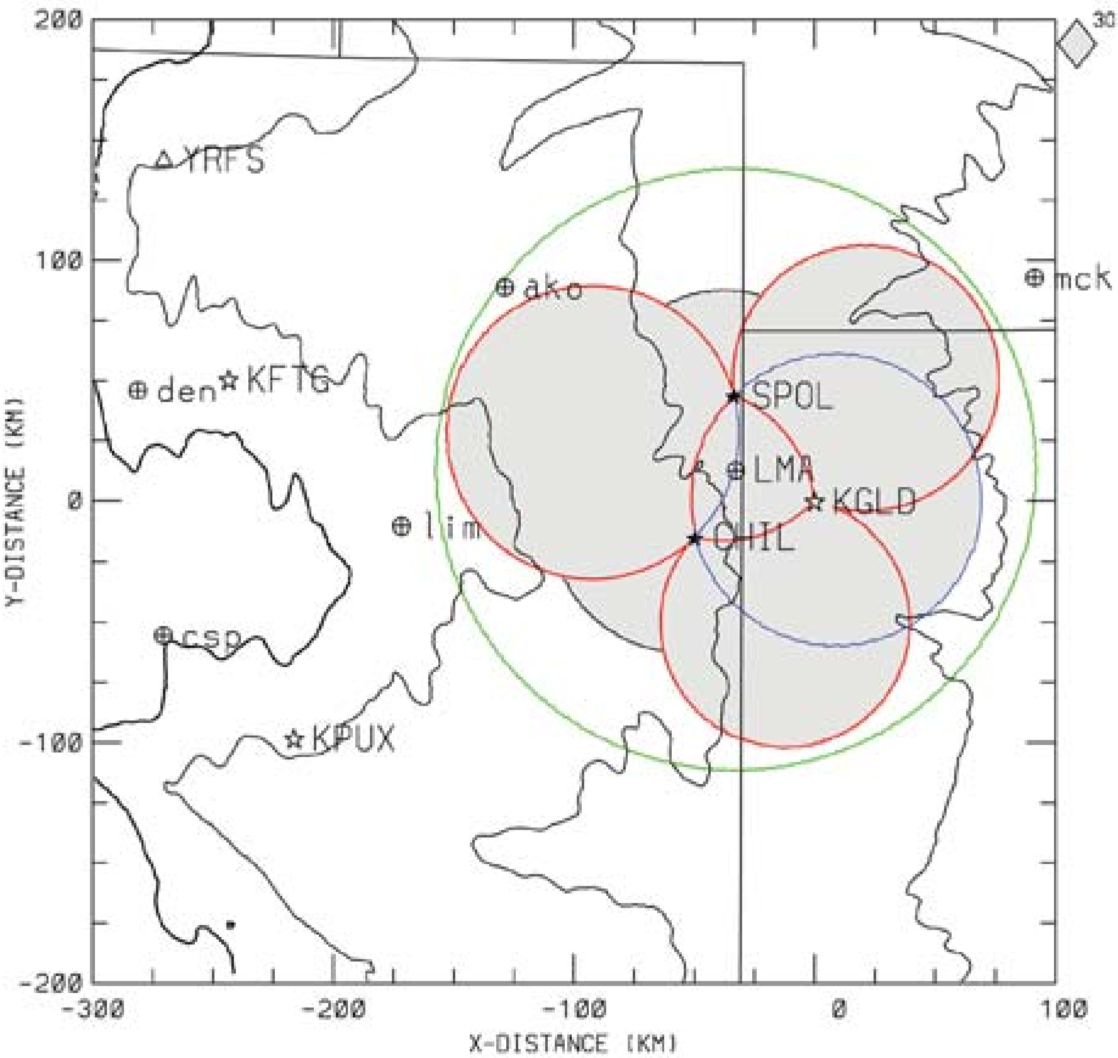

Fig. 3.1: Setup of the STEPS network over the High Plains. Dual-Doppler lobes are outlined in red, the dual-Doppler lobe between CHILL and S-Pol is outlined in blue, and the region with vertical resolution better than 1 km is outlined in green, about a 125 km radius. Terrain contours are black. LMA label denotes center of LMA network. From Lang et al. (2004).

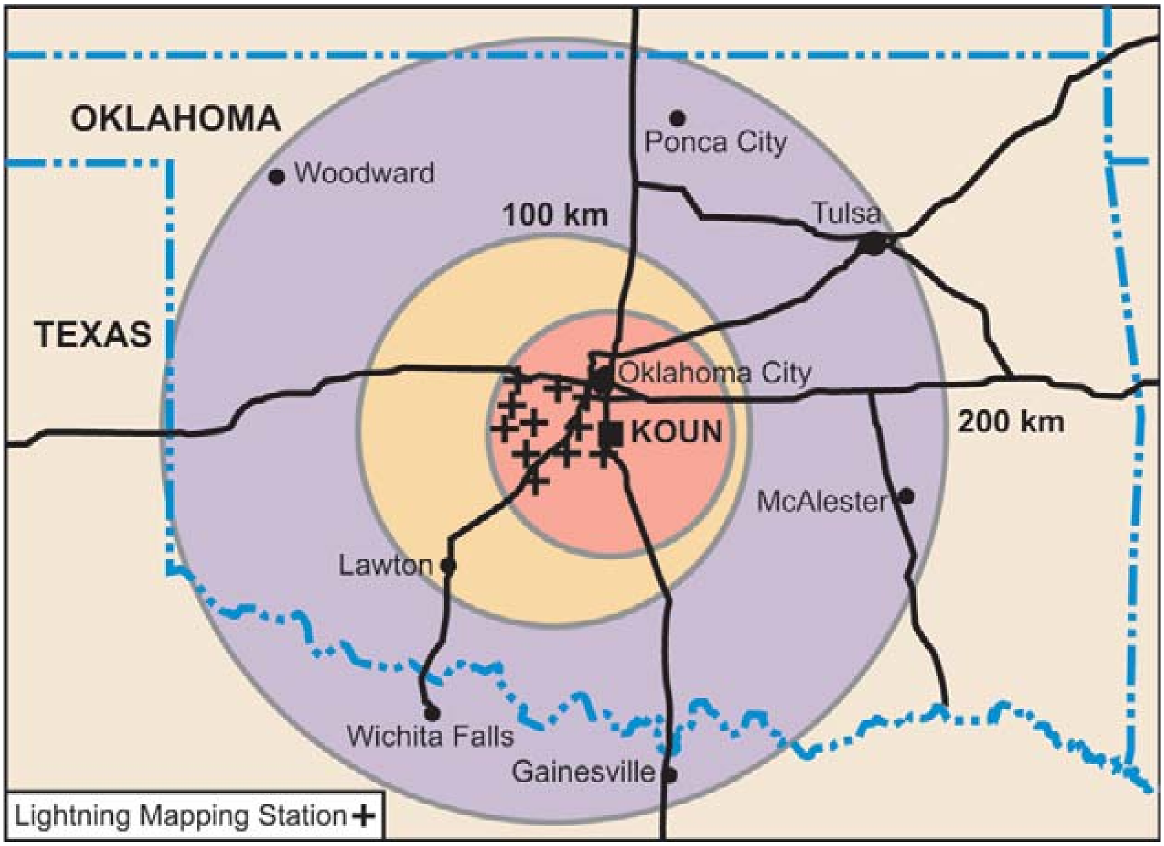

Fig. 3.2: Setup of the TELEX network over central Oklahoma. Red shading gives a 60 km radius around KOUN. Gold shading gives a 100 km radius around the LMA (black crosses) where lightning could be mapped well in three dimensions. Purple shading gives the 200-km nominal range around the LMA where lightning could be mapped in two dimensions. From MacGorman et al. (2008).

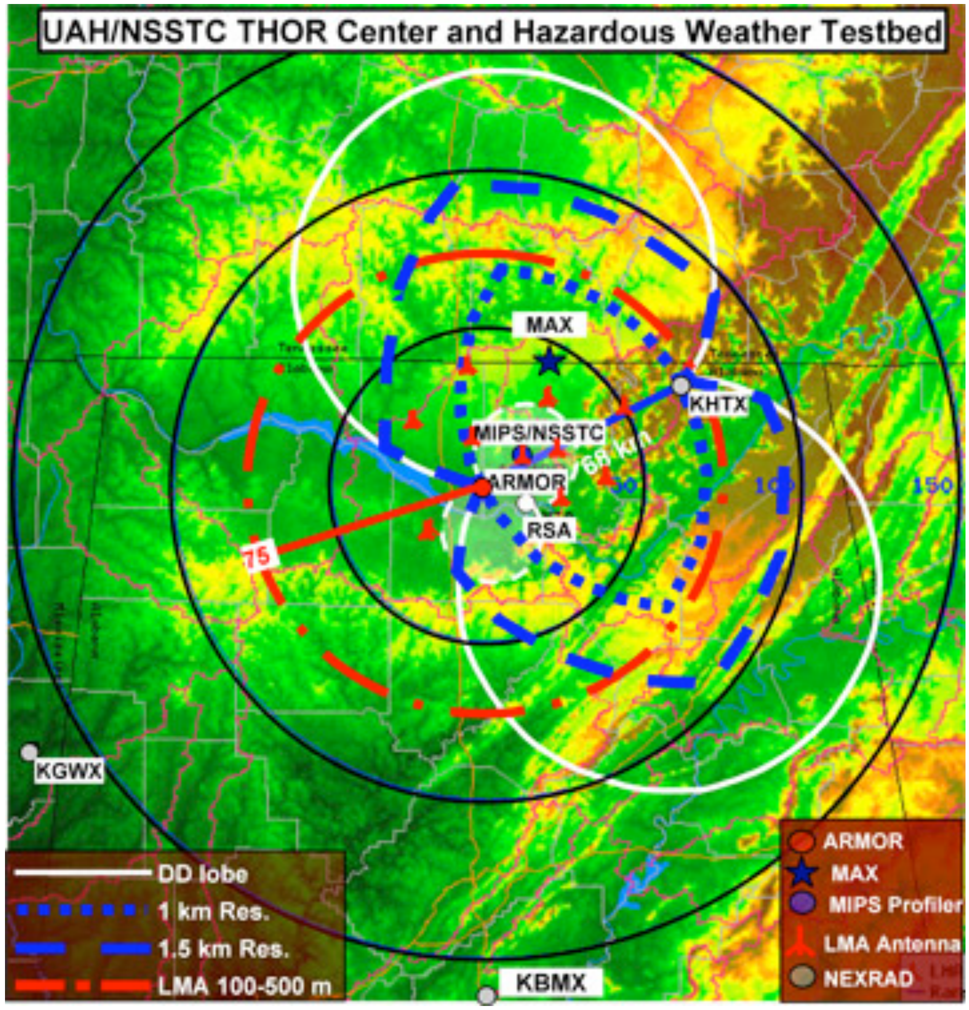

Fig. 3.3: UAH/NSSTC Hazardous Weather Tested setup. ARMOR radar is located towards the center of the image. LMA network is shown as red triangles. The white and dashed blue lines represent dual-Doppler lobes between ARMOR and the NWS Hytop radar (KHTX). The red dash-dot line represents as 75-km radius around the LMA network. From NSSTC (2011).

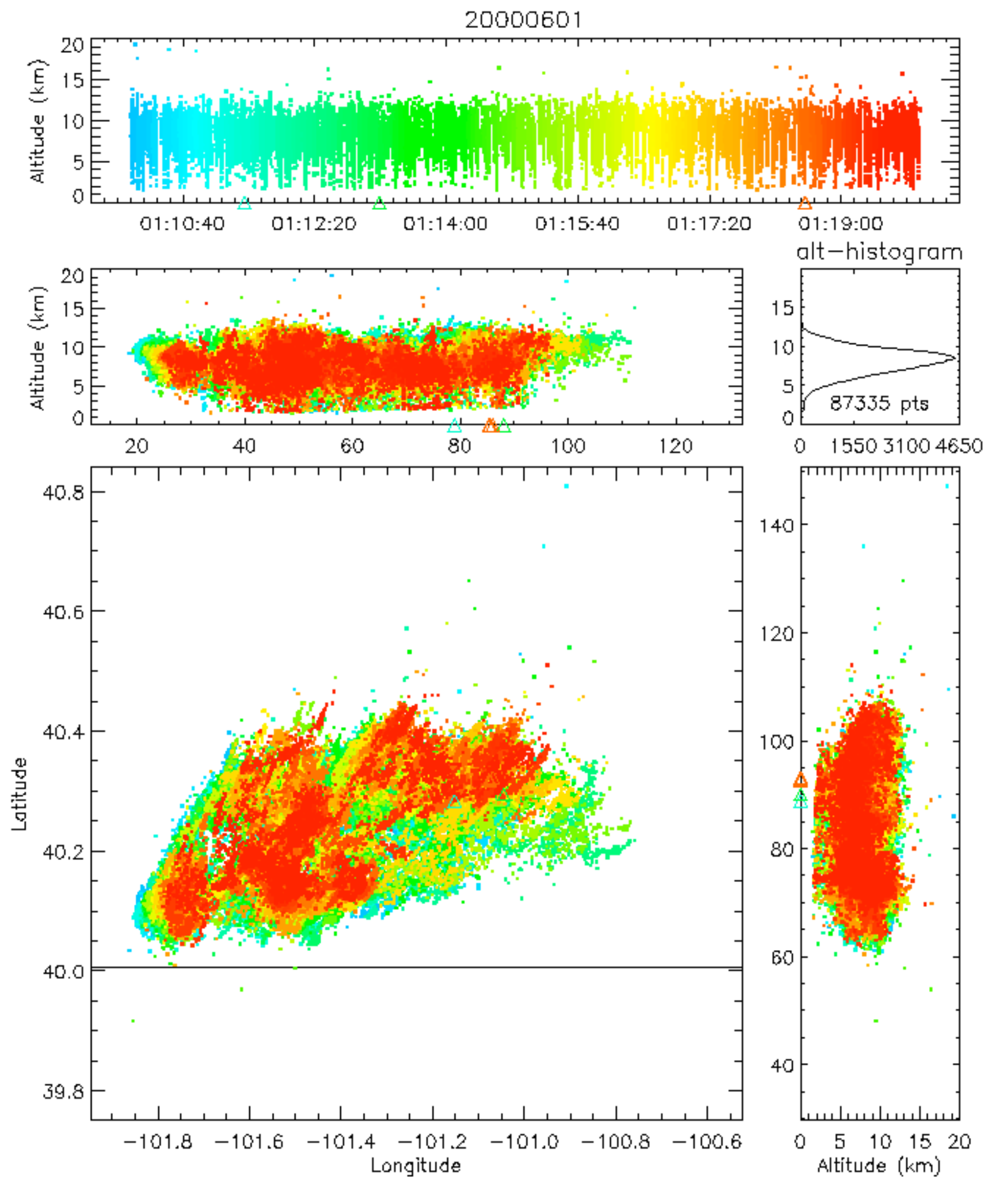

Fig. 3.4: Example of the XLMA interface.

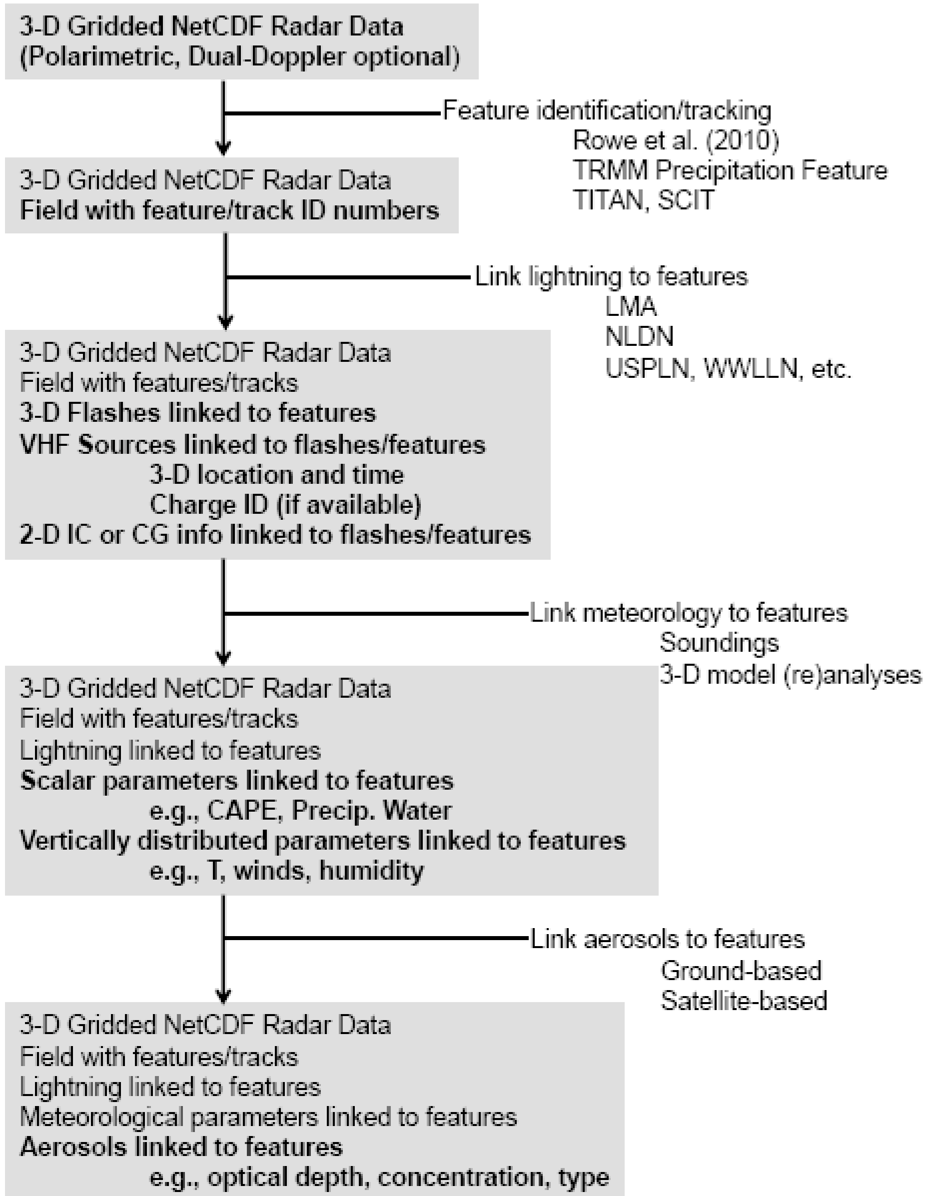

Fig. 3.5: Schematic of the CLEAR framework. Each addition to the main radar file is shown in a gray shaded box. Feature identification and tracking is performed, then lightning features, environmental features and aerosol features (not used in this study) are added to the tracked radar features. From Lang and Rutledge (2011).

CHAPTER 4

Brief overview of storms

For this study, seven storms were considered from three climatically different locations: the relatively more arid and higher-sheared environment of the western High Plains, the moist, highly-sheared environment of central Oklahoma, and the lower shear, moist sub-tropical environment of northern Alabama (Fig. 4.1). A brief description of each storm is provided here. Storm characteristics are summarized in Table 4.1 and example storm images found in Fig. 4.2. For this study, a storm is defined as +CG (-CG) dominant if, over the course of its observed period, over 50% of the CG flashes were positive (negative).

4.1 31 May 2000

The 31 May 2000 storm (Fig. 4.1a) formed as a low precipitation supercell in the High Plains area of northeastern Colorado (see Lang et al. 2004 for this and the other High Plains storms). Conditions on this day consisted of a surface low over eastern Colorado and upper-level trough approaching from the west with pre-storm dewpoints around 13 °C. Observations of this storm by instruments in the STEPS field experiment lasted approximately two hours until it approached the edge of the observation network. During the observing period, this storm was approximately 100 to 125 km from the center of the LMA network moving towards the northeast. This storm was +CG dominant for the entire observing period.

4.2 24 June 2000

The 24 June 2000 storm (Fig. 4.1b) formed as a classic supercell in the High Plains of northeastern Colorado and was observed by the STEPS network. There was a weak upper-level wave moving through western Colorado and low dewpoints near 4 °C and slight upslope winds. Observations lasted approximately three hours through most of the life cycle of the storm, and the storm moved from approximately 120 km to 80 km from the center of the LMA network moving towards the east-southeast. It was +CG dominant through most of its observed lifetime, with a higher magnitude of both +CG percentage and +CG flash rate at the end of its life.

4.3 5 July 2000

The 5 July 2000 storm (Fig. 4.1c) was a low-precipitation supercell that formed in the far northeast corner of Colorado and was observed by the STEPS network. Conditions included an upper-level trough over the West Coast and a dryline over eastern Colorado with upslope surface winds. Observations lasted approximately two and one-half hours until the cell moved out of the observation area. During this time, the storm was approximately 60 to 125 km from the center of the LMA network moving towards the east-northeast. This cell was +CG dominant for most of its observed lifetime and was discussed in detail by Lang et al. (2004) and MacGorman et al. (2005).

4.4 26 May 2004

The 26 May 2004 storm (Fig. 4.1d) formed in west-central Oklahoma as a classic supercell and was observed by the TELEX network for approximately three hours. Conditions included the upper-level jet stream positioned across northern Oklahoma and a dryline across western Oklahoma just east of the panhandle with surface dewpoints approaching 21 °C. The storm was initially too far away from the observing network, but then moved into the network (about 125 km from the LMA center) from the west before dissipating just to the west of the KOUN radar and over the LMA network. Therefore, only the latter half of its lifetime was observed and useable for this study. It was -CG dominant at the beginning of observations, becoming +CG dominant as it began to dissipate. This storm was examined in other papers, e.g., MacGorman et al. (2008) and Bruning et al. (2010).

4.5 29 May 2004

The 29 May 2004 storm (Fig. 4.1e) formed in west-central Oklahoma as a high precipitation supercell observed by the TELEX network. Conditions for this case included a negatively-tilted upper-level trough moving in from the west and a dryline near the border of Oklahoma and the Texas Panhandle with dewpoints east of the dryline approaching 21 °C. The storm itself lasted over 10 hours, and observations were available from close to the beginning of its lifetime out to almost 7 hours. Distance from the LMA network varied from approximately 125 km to 100 km, then back out past 125 km and out of the network as the storm moved towards the east. The storm was highly -CG dominant (with less than five percent +CG flashes) and produced a large amount of lightning. This storm has been examined in detail in other papers, such as MacGorman et al. (2008) and Payne et al. (2010).

4.6 3 May 2006

The 3 May 2006 storm (Fig. 4.1f) formed in northern Alabama as a severe multicell that moved southward towards the ARMOR radar and LMA network and was observed for approximately 1.5 hours. Conditions included a weak upper-level wave over Louisiana and surface dewpoints around 15 °C. The storm began approximately 50 km from the LMA center, moving to directly over the LMA network at the end of the observing period from the north. This storm presented a different type of storm than the other supercells, which were single-cellular compared to the multicellular structure of this case, and was -CG dominant through the entire observing period.

4.7 3 April 2007

The 3 April 2007 storm (Fig. 4.1g) formed in northern Alabama as a non-tornadic supercell and was observed by the ARMOR radar and LMA network starting at the beginning of its life cycle for approximately two hours. This storm formed ahead of a strong surface cold front and associated squall line. The storm began approximately 50 km from the LMA network center and moved to the east to approximately 100 km from the center. It was -CG dominant throughout the observing period.

Table 4.1: Storm characteristics.

Date	Storm type	Max percent +CG	Obs period (UTC)	Field program
31 May 2000	Low precipitation supercell	73	0038-0229	STEPS
24 Jun 2000	Classic supercell/severe multicell	96	0005-0303	STEPS
05 Jul 2000	Low precipitation supercell	93	2252-0129	STEPS
26 May 2004	Classic supercell	39	2155-0058	TELEX
29 May 2004	Tornadic high precipitation supercell	14	2002-0734	TELEX
03 May 2006	Severe multicell	2	2103-2223	none
03 Apr 2007	Non-tornadic supercell	6	1854-2044	none

Fig. 4.1: General map of the three regions examined in this thesis.

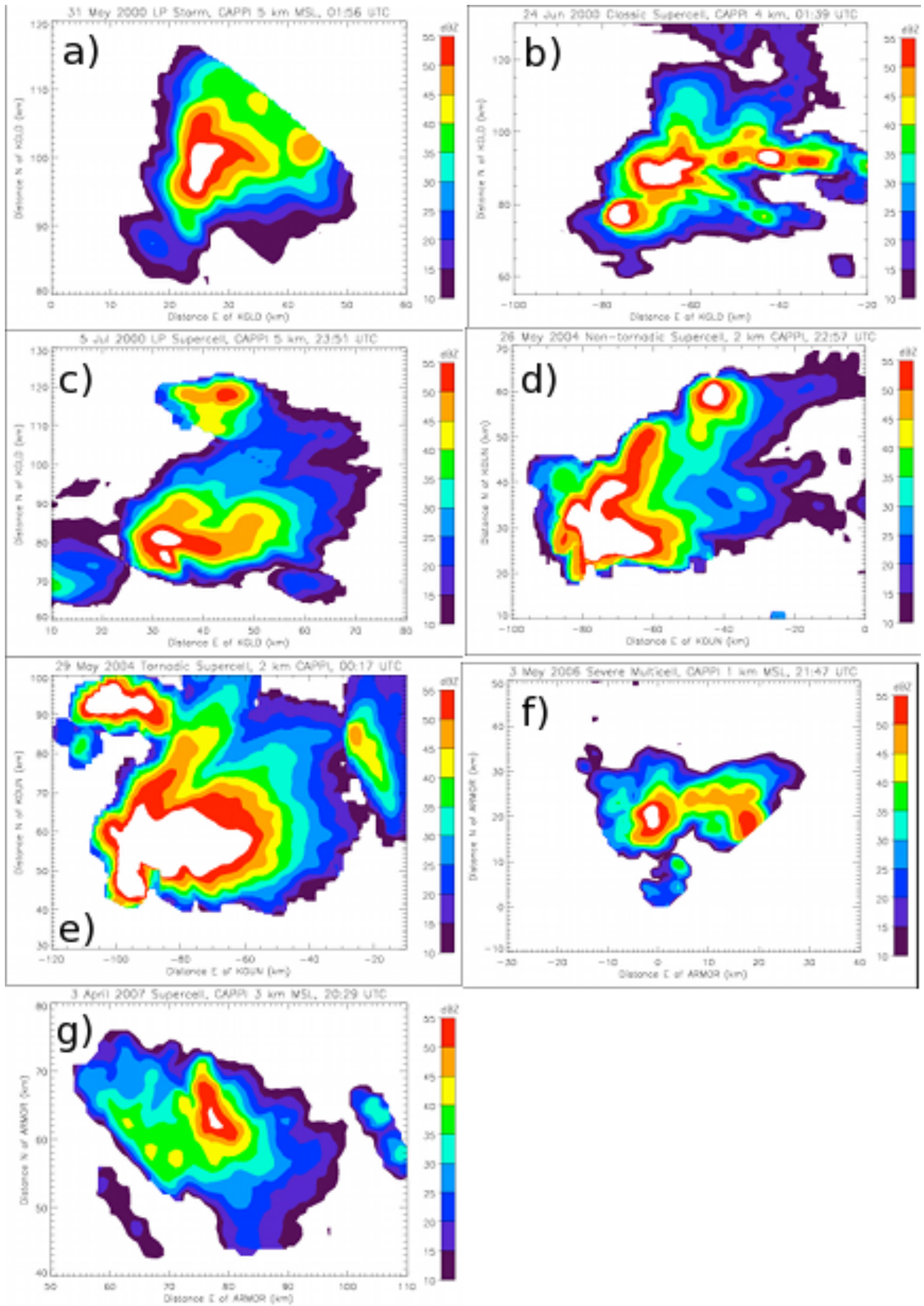

Fig. 4.2: Example radar returns for storms on (a) 31 May 2000, (b) 24 June 2000, (c) 5 July 2000, (d) 26 May 2004, (e) 29 May 2004, (f) 3 May 2006, and (g) 3 April 2007, displayed on a Constant Altitude Plan Position Indicator (CAPPI).

CHAPTER 5

Results

5.1 Comparison between regions

The High Plains storms were +CG dominant and the Oklahoma and Alabama storms were -CG dominant except for the 26 May 2004 storm, which transitioned to +CG dominant towards the end of its lifetime. Because the switch to +CG dominance occurred during dissipation, it is possible that different mechanisms contributed to the CG polarity in this case compared to the High Plains storms, such as a collapsing updraft as described in Wiens (2005) or as described in the Bruning et al. (2010) study of this storm, which advanced that an inverted charge structure developed based on the separation of lighter, negatively charged graupel from heavier, positively charged graupel and hail. This stratification of +CG and -CG dominance means that comparing the environments, stratified by region, could possibly indicate differences/similarities between +CG and -CG dominant storms as well as differences in regional meteorology. Thus, various RUC-estimated environmental parameters assigned via the statistical framework from the RUC reanalysis were examined.

Table 5.1 gives the mean values for each storm of several environmental parameters representing wind structure and thermodynamic elements in the atmosphere. As described in Section 3.4, these parameters are taken to be representative of the pre-storm, or upstream, environment as a mean over its lifetime. Overall, there were no major differences between environmental parameters between these storms by region. Regarding instability, there is considerable spread in CAPE and CIN between the storms, particularly among the High Plains storms where CAPE ranged from 843 to 5542 J kg^{-1} and CIN ranged from -45 to -276 J kg^{-1}. The Oklahoma and Alabama storms' instability values were more consistent with each other, with the Oklahoma environments having higher CAPE and CIN values compared to the Alabama environments, although both of these fell within the ranges of the High Plains environments. Moisture values were also mostly consistent among the regions, with the Oklahoma and Alabama environments once again falling within the range of the High Plains environments in dewpoint and relative humidity values. One notable difference is the near-surface relative humidity of the 24 June 2000 storm, which was only 39%, much lower than the 61-68% range of the other cases. When considering θ_e, the Oklahoma environments once again fall within the range of the High Plains environments. The Alabama values are slightly lower than the other storms but by only 2 K. Values of the 0-6 km wind shear were slightly higher for the Oklahoma environments than the High Plains, with the Alabama environments being the lowest. Although the wind shear could be stratified by region in this way, the difference between the highest Alabama and lowest High Plains shear was only 1 m s^{-1}, and the difference between the highest High Plains shear and lowest Oklahoma shear was only 2 m s^{-1}. As with θ_e, these differences were too small to draw any meaningful physical conclusions. The 0-3 km storm relative helicity was also examined. The Oklahoma environments fell within the spread of the High Plains environments, and the Alabama environments had slightly lower values of storm relative helicity than the other two regions. Again, the difference was not large enough (15 m^2 s^{-2} between lowest High Plains and highest Alabama values) to draw any conclusions. Bulk Richardson numbers were similar across the storm environments as well (Table 2), with the 3 May 2006 multicell storm having the highest value. Warm cloud depth (difference between cloud base and freezing level heights) was examined as well. Overall, all the storms had similar warm cloud depths between 3 and 3.5 km, with the exception of the 24 June 2000 storm, which had a warm cloud depth of only 1.73 km.

Due to the small sample size, the lack of patterning in environmental variables between regions does not show definitively that there would be no statistically significant differences between the regions with larger datasets. Additionally, the RUC was used to classify the environment for these cases, and it is possible that direct observations with pre-storm soundings would provide a more accurate and possibly different picture. However, this finding does imply that there are no clearly defined factors between the storms in different regions that are apparent for every case, and it is possible that there are multiple combinations of conditions that could lead to +CG dominant storms. These particular combinations could be highlighted by a statistical analysis of a larger dataset.

Another important finding was that there were no warm-cloud depth differences between the High Plains +CG cases and the Oklahoma and Alabama -CG cases. A comparison of warm cloud depths for each case for the different regions is shown in Fig. 5.1. A smaller warm-cloud depth was advanced as an explanation for the increased occurrence of +CG dominant storms in the High Plains by Williams et al. (2005), a finding which was supported by Carey and Buffalo (2007). Due to the small sample size, the results here do not refute that hypothesis, but they also do not support them and suggest that in some conditions, such as those that led to the storms in this study, other mechanisms are at work in producing inverted polarity storms that are +CG dominant.

5.2 Comparison between +CG and -CG dominant storms

For each storm, VHF source density from the LMA observations was plotted as a function of height (in temperature coordinates) and time (Fig. 5.2a-b). Temperature was chosen as the height coordinate in order to make a more representative comparison between the different climates and elevations of the three regions. In these figures, the layer of maximum source density (shown in white) is inferred to be associated mainly with negative leaders discharging a positive charge layer in each storm (Rison et al. 1999). This inference of location of the positive charge layer of the storm can be made because the LMA is more sensitive to VHF radiation produced by negative charge propagating through areas of positive space charge, compared to positive charge propagating through areas of negative charge (Mazur et al. 1997). This concept was used to infer storm structure in Rust et al. (2005) and Wiens et al. (2005), and other studies as well. For the +CG dominant storms of 31 May 2000, 24 June 2000, and 5 July 2000, the maximum in source density, inferred as the approximate position of the positive charge layer, is at a warmer temperature (lower height) than that of the -CG dominant storms of 29 May 2004, 3 May 2006, and 3 April 2007. The 26 May 2004 storm was first observed as a -CG dominant storm that transitioned to a +CG dominant storm at the end of its lifetime. In line with the result of maximum source density height between +CG and -CG dominant storms, the 26 May 2004 storm's level of maximum source density began at colder temperatures (higher heights) and transitioned to warmer temperatures (lower heights) when the storm transitioned to +CG dominance. This can be seen in Fig. 5.2a at approximately 2330 UTC. Overall, the +CG storms' maximum source density occurred at an average -24 °C while -CG storm's maximum source density occurred at an average -37 °C, a difference of 13 °C. The warmer temperature (lower height) of the maximum source density level in the +CG storms examined here suggests an inverted charge structure in these storms (Rust et al. 2005), while the colder temperature (higher height) in the -CG dominant storms suggests a normal-polarity structure, with a positive charge layer over mid-level negative charge (Williams 1989). These results support the conclusions of several studies such as Wiens et al. (2005), Tessendorf et al. (2007), and Rust et al. (2005), which found that an inverted charge structure, with upper-level and lower-level negative charge over mid-level positive charge, occurred in many cases of +CG dominant storms. This also supports the finding in Lang et al. (2004) specifically regarding the 5 July 2000 storm, which found indications of inverted polarity for that case. Lang and Rutledge (2011) also found that the positive charge layer occurred lower in +CG dominant storms than -CG dominant storms during STEPS.

This result suggests that an inverted charge structure results in, or is at least correlated with, +CG dominant storms, which leads to the next research step of determining what mechanism(s) may produce the inverted structure. Although this study cannot draw any rigid conclusions due to the small number of cases studied, several parameters were examined to determine if there were any differences between the +CG and -CG storms in terms of structure. Environment was also examined, but as was presented in the previous subsection, there were no clearly defined differences between the environments of the +CG dominant storms and the -CG dominant storms, aside from the well-documented fact that +CG dominant storms are more prolific in the High Plains than in the Southeast (Orville et al. 2002). This is in contrast to Lang and Rutledge (2011), which suggested that +CG dominant storms during STEPS were associated with environments that favored more intense convection.

Using the dual-Doppler analysis described in Chapter 3, updraft characteristics of six of the seven storms were examined (no dual-Doppler analysis was available for 29 May 2004 for this study). A major difference between the storms' updraft volumes was observed. To control for differences in storm volume between each case, updraft volumes as percent of total storm volume were compared. The updraft volume itself was defined as updrafts of >10 m s^{-1}, the speed where the updraft would be relatively free from entrainment and liquid water contents would approach adiabatic levels, as in the precipitation growth model used by Knight and Knupp (1986). Figure 5.3 shows the overall results of this analysis. The three High Plains storms, all +CG dominant, had much larger updraft volumes as percent of total storm volume than the -CG dominant storms. Overall, the +CG storms (31 May 2000, 24 June 2000, 5 July 2000) had an average >10 m s^{-1} updraft volume that was 9.69% of the total storm volume, whereas the -CG dominant storms (26 May 2004, 3 May 2006, 3 April 2007) had an average >10 m s^{-1} updraft volume that was just 0.34% of the total storm volume, with the 3 April 2007 storm having no updraft volume above 10 m s^{-1}. Lang et al. (2004) found a strong updraft in the 5 July 2000 supercell as well as another +CG dominant cell during STEPS and suggested a possible link between the strong updrafts and +CG dominance, and this appears support in this study. As discussed in Williams (2001) and Wiens et al. (2005), a broad updraft such as those found in the +CG dominant STEPS storms in this study would be less impacted by entrainment, allowing supercooled liquid water contents to approach adiabatic values in the mixed-phase region of the updraft. Laboratory studies of non-inductive charging (e.g., Takahashi 1978; Saunders and Peck 1998) suggest that graupel would acquire a positive charge in environments of high liquid water content, settling in the mid-levels of the storm while the negatively charged, lighter crystals would be carried to upper levels. It is possible that the updrafts in the +CG dominant storms in this study, which exhibited much larger volumes as a percentage of total storm volume compared to the -CG dominant storms, had some contribution to the inverted charge structure of these storms via producing large supercooled liquid water contents within the updraft.

There are two important caveats of this result to keep in mind. First, there was no second radar available for the 29 May 2004 storm with which a dual-Doppler analysis could be performed. This storm was the largest of the cases studied here as well as the most prolific lightning producer (MacGorman et al. 2008). It would follow that the 29 May 2004 storm also had a large updraft, as discussed in Payne et al. (2010) in relation to a lightning hole around the bounded weak echo region (BWER), and it remains a question how large the updraft was in relation to the rest of the cell and whether this -CG dominant storm would also have a smaller updraft volume as percent of total volume as the other -CG dominant storms in this study. Second, the sample size is very small for this set of storms, so the results cannot be generalized for all inverted or +CG dominant storms. However, the results are worth investigating further, and CLEAR may provide a way to do this with a large number of storms from a variety of datasets across these regions. Using STEPS cases, Lang and Rutledge (2011) found that +CG dominant storms were larger and more vertically developed than -CG dominant storms, implying larger updrafts. Also, for this analysis, the 26 May 2004 storm was considered -CG dominant. The transition to +CG dominance occurred as the storm was dissipating, and therefore the storm's updraft was dissipating, indicating that its +CG dominance was possibly caused by a different mechanism than the High Plains storms. One possible mechanism is that the collapsing updraft allowed the upper-level positive charge layer to fall to mid-levels as with a storm described by Wiens (2005). Another possible mechanism was advanced by Bruning et al. (2004), which suggested that the inverted charge structure resulted from the separation of lighter, negatively charged graupel from heavier, positively charged graupel and hail.

There is also some indication that larger graupel echo volumes are associated with an inverted charge structure and +CG dominance in these storms. In Fig. 5.4, it is seen that the High Plains storms with their lower altitude positive charge layer tended to have slightly larger graupel echo volumes as a percentage of total storm volume. This may relate back to the larger, broader updrafts of these storms described earlier in this section, which would limit entrainment and provide larger supercooled liquid water contents for the graupel to grow within.

Table 5.1: Mean values for environmental variables for each storm.

	High Plains			Oklahoma		Northern Alabama	
	31 May	24 Jun	5 Jul	26 May	29 May	3 May	3 Apr
CAPE (J kg^{-1})	977	843	5542	3975	3727	1225	1275
CIN (J kg^{-1})	-276	-45	-61	-72	-80	-21	-17
Dewpoint (°C)	22	20	27	24	24	20	19
RH (%)	68	39	61	62	68	66	61
0-6 km shear (m s^{-1})	19	16	21	28	23	7	15
0-3 km SRH (m^2 s^{-2})	661	149	361	159	359	55	134
Theta-e (K)	340	342	367	359	358	339	338
Warm cloud depth (km)	3.42	1.73	3.23	3.57	3.54	2.80	3.14
Bulk Ri	2.7	3.2	12.8	5.2	7.1	26.7	5.9

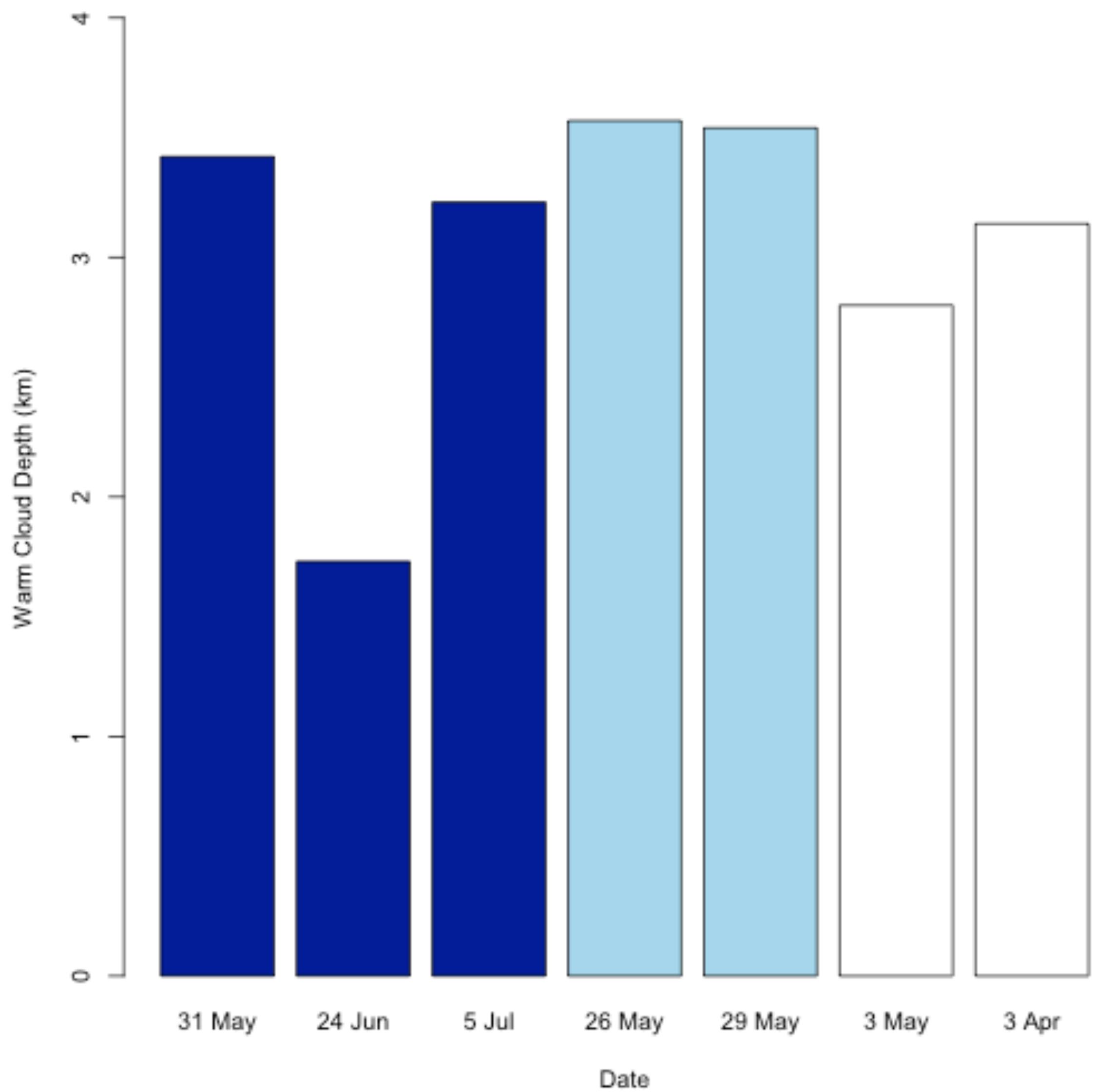

Fig. 5.1: Mean warm cloud depth by case. High Plains storms are shown in dark blue, central Oklahoma storms in light blue, and northern Alabama storms in white.

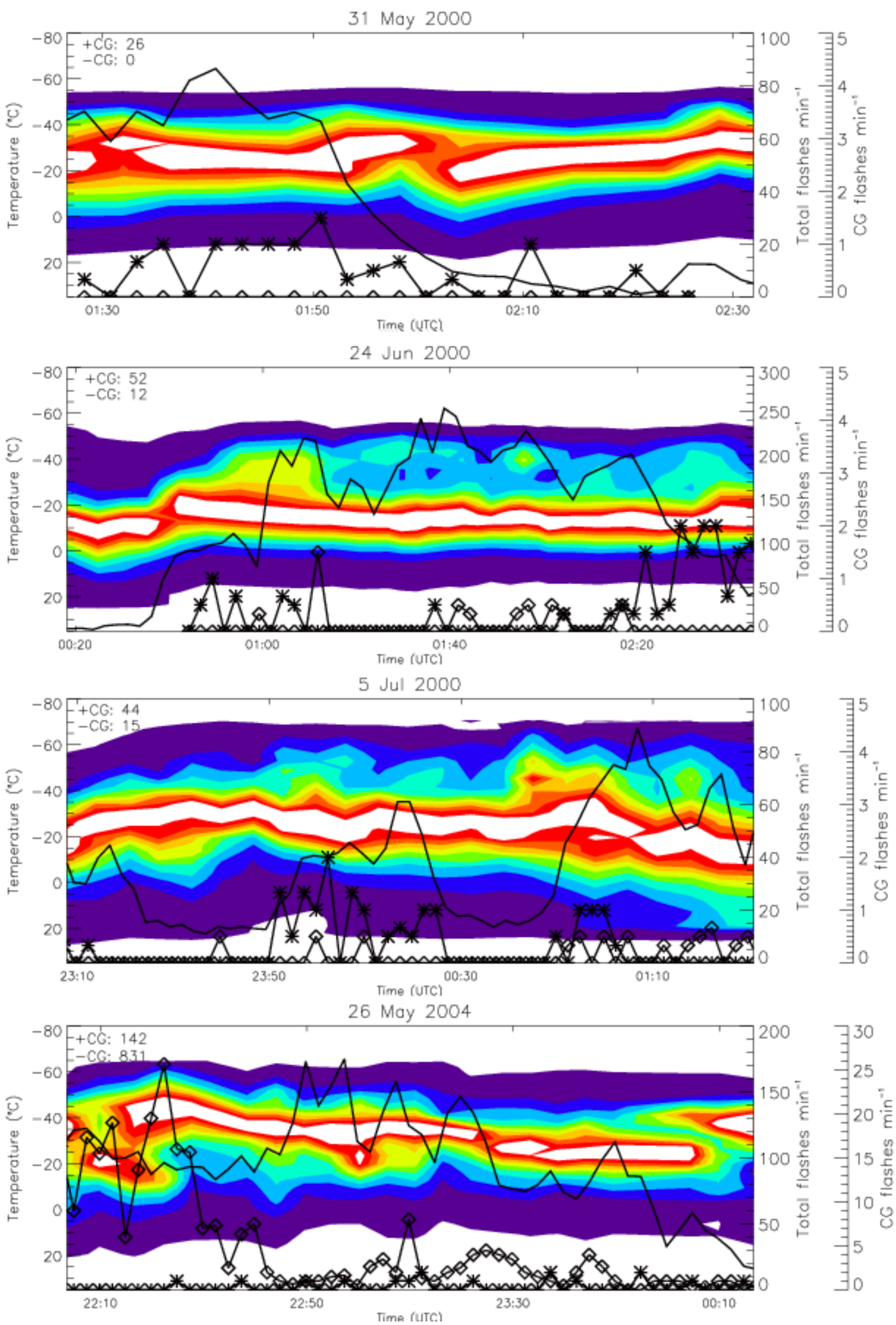

Fig 5.2a: Lightning characteristics for each storm. LMA source density as percentage of maximum source density in volume scan is shown in color filled contours (1 to 100% every 10%), total lightning flash rate as solid black line, and both +CG and -CG flash rates as connected asterisks and diamonds, respectively. Total number of +CG and -CG flashes shown in upper left corner.

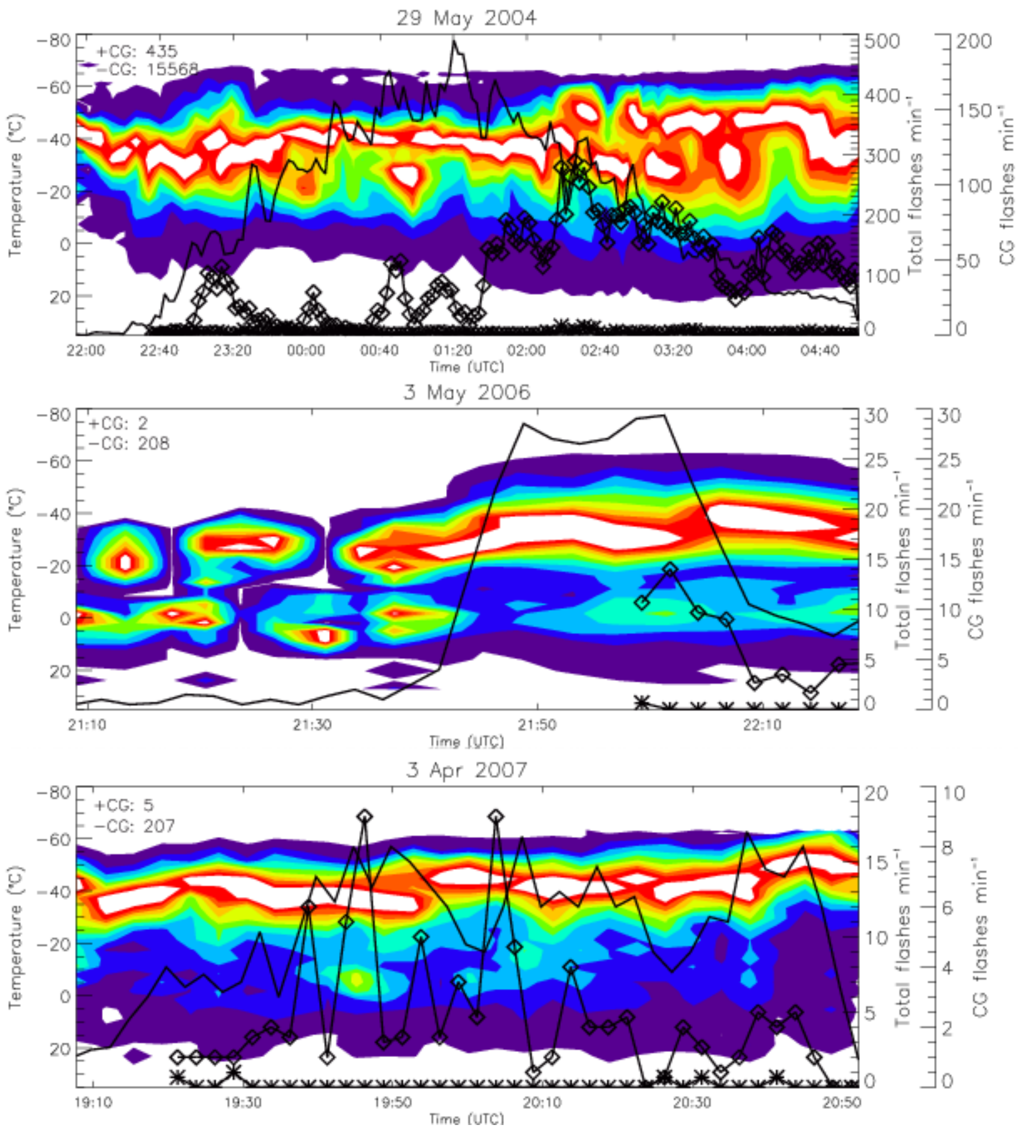

Fig. 5.2b: Same as Fig. 5.2a, for remaining storms.

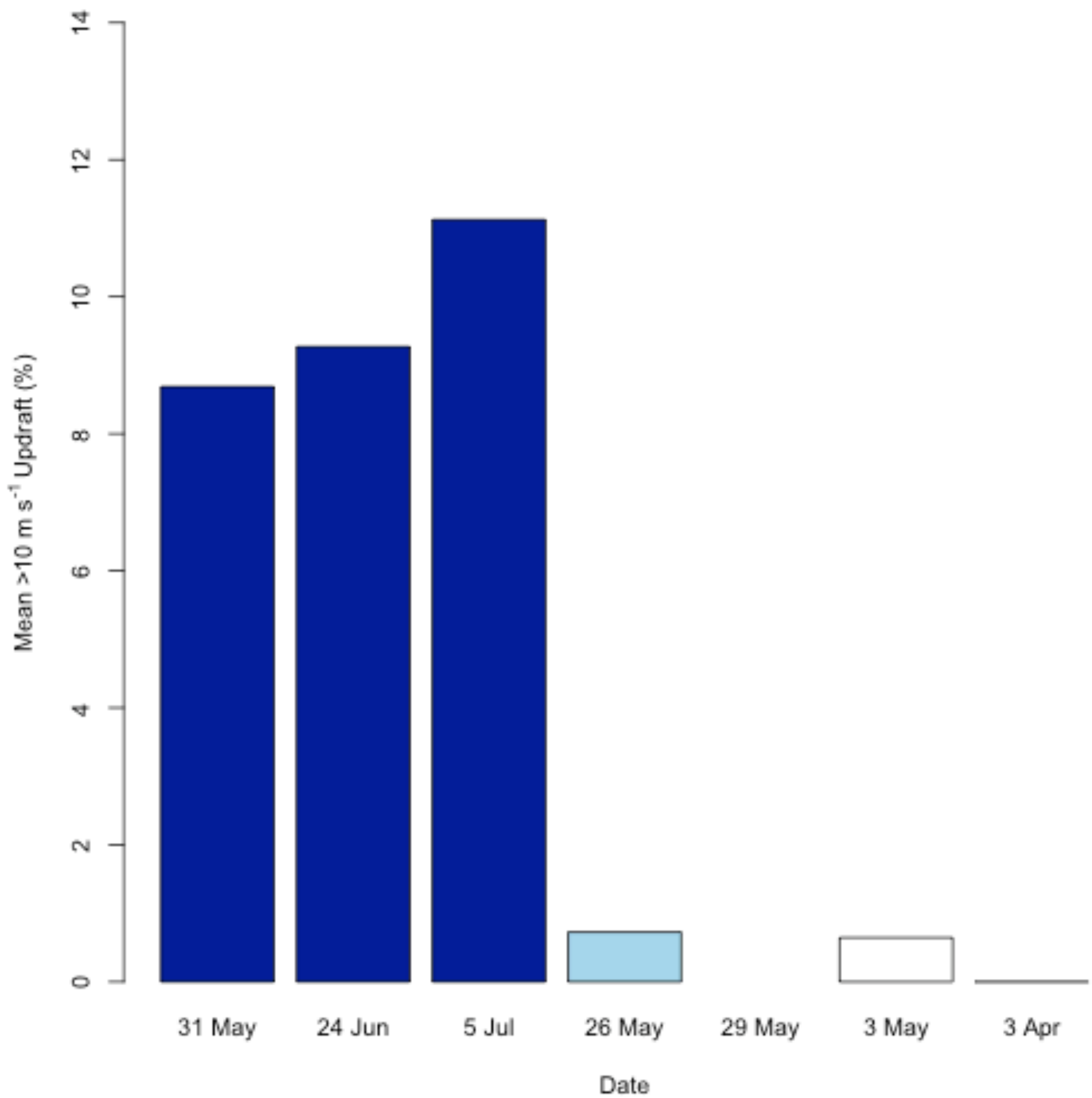

Fig. 5.3: Mean updraft (> 10 m s^{-1}) volume as percent of total storm volume for each case for volume scans where dual-Doppler analysis was available. High Plains storms are shown in dark blue, Oklahoma storms in light blue, and northern Alabama storms in white. Note there was no updraft information available for 29 May 2004.

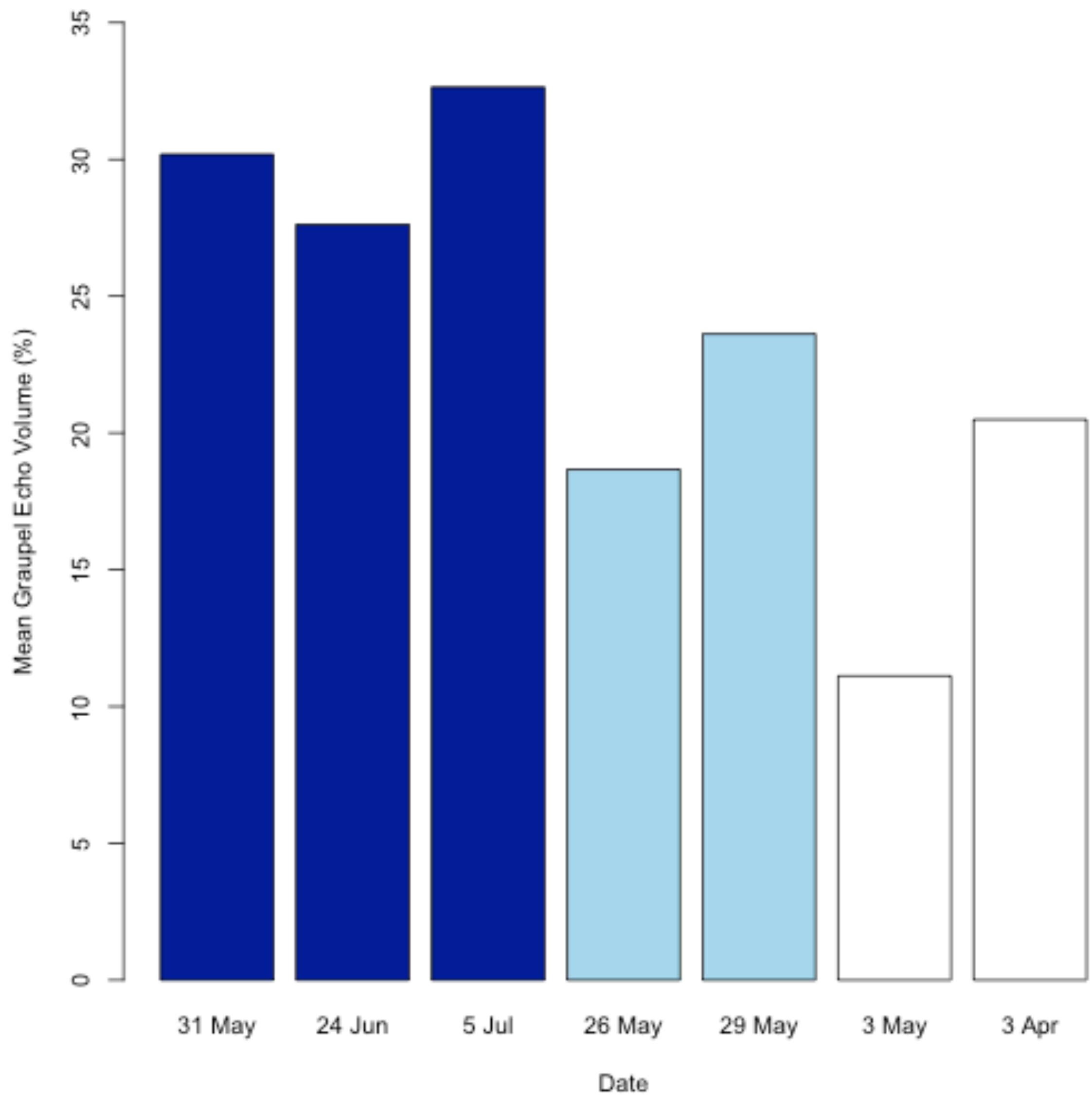

Fig. 5.4: Mean graupel echo volume as a percentage of total storm volume for each storm. High Plains storms are shown in dark blue, Oklahoma storms in light blue, and northern Alabama storms in white.

CHAPTER 6

Summary and conclusions

This study used an analysis framework called CLEAR (Lang and Rutledge 2011) to objectively examine seven storms from three different data sources. There were three +CG dominant and four -CG dominant storms from three different climatological regions: the High Plains, central Oklahoma, and northern Alabama. The storms were tracked using radar data, and total lightning and environmental characteristics were added to each storm cell automatically using CLEAR modules.

Comparing the environmental characteristics of storms from different regions or different CG polarity did not produce any meaningful differences between the cases. This included the depth of the warm-cloud layer, which has been advanced as a hypothesis for the larger percentage of +CG storms in Williams et al. (2005) and supported by Carey and Buffalo (2007). This small sample of storms does not refute those findings, but it does suggest that either more work must be done in investigating the role of warm-cloud depth, or that there could be multiple factors that influence CG polarity that do not always combine in the same way.

When stratifying the storms by CG polarity, there were three features that stood out. First, the level of the positive charge layer, as inferred by the level of maximum VHF source density, was at a much lower altitude (warmer temperature) in the +CG dominant storms than in the -CG dominant storms. In the 26 May 2004 storm, the transition from -CG dominant to +CG dominant was accompanied by a lowering of the positive charge layer. Second, the volume of the >10 m s^{-1} updraft of each storm, as a percentage of total storm volume, was much larger in the +CG dominant storms than in the -CG dominant storms. There was one exception in that the 26 May 2004 storm fell into the smaller updraft category, yet transitioned into a +CG dominant storm as it dissipated. This implies that the mechanisms producing a majority of +CG flashes in this dissipating storm were different than those producing the +CGs in the High Plains storms. One large question in this finding is the 29 May 2004 storm, which was a large -CG dominant storm that was not able to have dual-Doppler analysis performed with the data available at the time of this study. The larger, broader updrafts in the +CG dominant cases may lead to an inverted charge structure by limiting entrainment, which would promote higher liquid water contents and lead to positive charging of graupel and negative charging of smaller ice crystals. Finally, there is some indication that the +CG dominant storms contained larger amounts of graupel, possibly related to the broader updrafts and higher liquid water contents.

Overall, these results add additional credence to previous research into the inverted charge theory of +CG dominant storms. Not only did the +CG dominant High Plains storms exhibit inverted charge, but the 26 May 2004 storm also showed a lowering of the mean altitude of the inferred positive charge layer as it transitioned into a +CG dominant storm from a -CG dominant one. This study also indicates that the relative size of a storm's updraft may be a factor in whether a storm develops a normal or inverted charge structure. In addition to previous case study research (e.g., Wiens et al. 2005), similar results were obtained to the statistical analysis of STEPS storms presented in

Lang and Rutledge (2011), which provided a more robust statistical support of the inverted charge structure, the correlation with broad updrafts, and the lack of role played by warm-cloud depth using data spanning two months. In addition to these findings, this analysis used CLEAR to compare between different datasets in different regions, finding that in these cases there were no significant environmental differences between regions that appeared to have an impact on the storms' polarity.

Along with these findings of storm characteristics and environments, this study was able to use CLEAR to examine storms from different regions of the United States for which existed different types of datasets. In addition to statistical analysis of large datasets, the CLEAR framework proved useful in these case studies by combining the various radar, lightning, and environmental datasets into a common format that facilitated analysis.

A natural extension of this research would be to study a larger sample of thunderstorms from each of these different regions to determine what role the size of updraft plays in the development of inverted charge. Additionally, a large sample of storms from various locations may reveal a difference between the environment of storms that do and do not develop these large updrafts and improve understanding of how these different environmental parameters combine to form the broad updrafts in the +CG cases versus -CG cases.

REFERENCES

Benjamin, S. G., and Coauthors, 2004: An hourly assimilation–forecast cycle: The RUC. *Mon. Wea. Rev*, **132**, 495–518.

Bohne, A. R., and R. C. Srivastava, 1975: Random errors in wind and precipitation fall speed measurement by a triple Doppler radar system. University of Chicago Tech. Rep. 37, 50 pp.

Bruning, Eric C., W. David Rust, Donald R. MacGorman, Michael I. Biggerstaff, Terry J. Schuur, 2010: Formation of Charge Structures in a Supercell. *Mon. Wea. Rev.*, **138**, 3740–3761.

Brunkow, David, V. N. Bringi, Patrick C. Kennedy, Steven A. Rutledge, V. Chandrasekar, E. A. Mueller, Robert K. Bowie, 2000: A Description of the CSU CHILL National Radar Facility. *J. Atmos. Oceanic Technol.*, **17**, 1596–1608.

Carey, Lawrence D., Steven A. Rutledge, Walter A. Petersen, 2003: The Relationship between Severe Storm Reports and Cloud-to-Ground Lightning Polarity in the Contiguous United States from 1989 to 1998. *Mon. Wea. Rev.*, **131**, 1211–1228.

Carey, Lawrence D., Kurt M. Buffalo, 2007: Environmental Control of Cloud-to-Ground Lightning Polarity in Severe Storms. *Mon. Wea. Rev.*, **135**, 1327–1353.

Cummins, K. L., M. J. Murphy, E. A. Bardo, W. L. Hiscox, R. B. Pyle, and A. E. Pifer, 1998: A combined TOA/MDF technology upgrade of the U.S. National Lightning Detection Network. *J. Geophys. Res.*, **103** (D8), 9035–9044.

Dixon, M., and G. Wiener, 1993: TITAN: Thunderstorm identification, tracking, analysis, and nowcasting—A radar-based methodology. *J. Atmos. Oceanic Technol.*, **10**, 785–797.

Goodman, S. J., R. Blakeslee, H. Christian, W. Koshak, J. Bailey, J. Hall, E. McCaul, D. Buechler, C. Darden, J. Burks, T. Bradshaw, P. Gatlin, 2005: The North Alabama Lightning Mapping Array: Recent severe storm observations and future prospects. *Atmos. Res.*, **76**, 423-437.

Hubbert, J., V. N. Bringi, 1995: An Iterative Filtering Technique for the Analysis of Copolar Differential Phase and Dual-Frequency Radar Measurements. *J. Atmos. Oceanic Technol.*, **12**, 643–648.

Johnson, J. T., Pamela L. MacKeen, Arthur Witt, E. De Wayne Mitchell, Gregory J. Stumpf, Michael D. Eilts, Kevin W. Thomas, 1998: The Storm Cell Identification and Tracking Algorithm: An Enhanced WSR-88D Algorithm. *Wea. Forecasting*, **13**, 263–276.

Keeler, R. J., J. Lutz, and J. Vivekanandan, 2000: S-POL: NCAR's polarimetric Doppler research radar. Preprints, *IGARSS-2000*, Honolulu, HI, IEEE, 1570–1573.

Knight, C. A., and K. Knupp, 1986: Precipitation growth trajectories in a CCOPE storm. *J. Atmos. Sci.*, **43**, 1057–1073.

Lang, T. J., and Coauthors, 2004: The Severe Thunderstorm Electrification and Precipitation Study. *Bull. Amer. Meteor. Soc.*, **85**, 1107–1125.

Lang, T. J., and S. A. Rutledge, 2011: A framework for the statistical analysis of large radar and lightning datasets: Results from STEPS 2000. *Mon Wea. Rev.,* in press.

Liu, H., V. Chandrasekar, 2000: Classification of Hydrometeors Based on Polarimetric Radar Measurements: Development of Fuzzy Logic and Neuro-Fuzzy Systems, and In Situ Verification. *J. Atmos. Oceanic Technol.*, **17**, 140–164.

Lyons, Walter A., Marek Uliasz, Thomas E. Nelson, 1998: Large Peak Current Cloud-to Ground Lightning Flashes during the Summer Months in the Contiguous United States. *Mon. Wea. Rev.*, **126**, 2217–2233.

MacGorman, D. R., and W. D. Rust, 1998: The Electrical Nature of Storms. Oxford University Press, 422 pp.

MacGorman, D. R., W. D. Rust, P. Krehbiel, W. Rison, E. Bruning, K. Wiens, 2005: The Electrical Structure of Two Supercell Storms during STEPS. *Mon. Wea. Rev.*, **133**, 2583–2607.

MacGorman, D. R., and Coauthors, 2008: TELEX The Thunderstorm Electrification and Lightning Experiment. *Bull. Amer. Meteor. Soc.*, **89**, 997–1013.

Marzano, F. S., D. Scaranari, M. Celano, P. P. Alberoni, G. Vulpiani, M. Montopoli, 2006: Hydrometeor classification from dual-polarized weather radar: extending fuzzy logic from S-band to C-band data. *Advances in Geosciences*, **7**, 109-114.

Mazur, V., E. Williams, R. Boldi, L. Maier, and D. E. Proctor, 1997: Initial comparison of lightning mapping with operational time-of-arrival and interferometric systems. *J. Geophys. Res.*, **102**, 11, 07-11 085.

Mohr, C. G., L. J. Miller, R. L. Vaughn, and H. W. Frank, 1986: The merger of mesoscale datasets into a common Cartesian format for efficient and systematic analyses. *J. Atmos. Oceanic Technol.,* **3**, 143-161.

National Space Science and Technology Center (NSSTC), cited 2011: Storm – net. Available online at [http://nsstc.uah.edu/ARMOR/storm_net.html].

Orville, R. E., G. R. Huffines, W. R. Burrows, R. L. Holle, K. L. Cummins, 2002: The North American Lightning Detection Network (NALDN)—First Results: 1998 2000. *Mon. Wea. Rev.*, **130**, 2098–2109.

Oye, R., C. Mueller, and S. Smith, 1995: Software for radar translation, visualization, editing, and interpolation. Preprints, *27th Conf. on Radar Meteorology,* Vail, CO, Amer. Meteor. Soc., 359-361.

Payne, Clark D., Terry J. Schuur, Donald R. MacGorman, Michael I. Biggerstaff, Kristin M. Kuhlman, W. David Rust, 2010: Polarimetric and Electrical Characteristics of a Lightning Ring in a Supercell Storm. *Mon. Wea. Rev.*, **138**, 2405–2425.

Petersen, W. A., K. R. Knupp, L. D. Carey, D. Phillips, W. Deierling, and P. N. Gatlin, 2009: The UAH/NSSTC Advanced Radar for Meteorological and Operational Research (ARMOR). *34th Conf. on Radar Meteorology,* Williamsburg, VA, Amer. Met. Soc., P8.5.

Rison, W., R. J. Thomas, P. R. Krehbiel, T. Hamlin, and J. Harlin, 1999: A GPS-based Three-Dimensional Lightning Mapping System: Initial Observations in Central New Mexico. *Geophys. Res. Lett.*, **26**, 3573-3576.

Rowe, A. K., S. A. Rutledge, and T. J. Lang, 2011: Investigation of microphysical processes in isolated convection in NAME. *Mon. Wea. Rev.*, **139**, 424-443.

Rust, W. D., and D. R. MacGorman, 2002: Possibly inverted-polarity electrical structures in thunderstorms during STEPS. *Geophys. Res. Lett.*, **29**, 1571.

Rust, W. D., D. R. MacGorman, E. C. Bruning, S. A. Weiss, P. R. Krehbiel, R. J. Thomas, W. Rison, T. Hamlin, and J. Harlin, 2005: Inverted-polarity electrical structures in thunderstorms in the Severe Thunderstorm Electrification and Precipitation Study (STEPS). *Atmos. Research*, **76**, 247-271.

Ryzhkov, A. V., T. J. Schuur, D. W. Burgess, P. L. Heinselman, S. E. Giangrande, and D. S. Zrnić, 2005: The Joint Polarization Experiment: Polarimetric rainfall measurements and hydrometeor classification. *Bull. Amer. Meteor. Soc.*, **86**, 809 824.

Saunders, C. P. R., and S. L. Peck, 1998: Laboratory studies of the influence of the rime accretion rate on charge transfer during graupel/crystal collisions. *J. Geophys. Res.*, **103**, 13949–13956.

Smith, S. B., J. G. LaDue, D. R. MacGorman, 2000: The Relationship between Cloud-to Ground Lightning Polarity and Surface Equivalent Potential Temperature during Three Tornadic Outbreaks. *Mon. Wea. Rev.*, **128**, 3320–3328.

Storm Prediction Center, cited 2008: Severe Weather Event Summaries. Available online at [http://www.spc.noaa.gov/climo/online/]

Straka, J. M., D. S. Zrnić, and A. V. Ryzhkov, 2000: Bulk hydrometeor classification and quantification using polarimetric radar data: Synthesis of relations. *J. Appl. Meteor.*, **39**, 1341–1372.

Takahashi, T., 1978: Riming electrification as a charge generation mechanism in thunderstorms. *J. Atmos. Sci.*, **35**, 1536–1548.

Tessendorf, S. A., L. J. Miller, K. C. Wiens, S. A. Rutledge, 2005: The 29 June 2000 Supercell Observed during STEPS. Part I: Kinematics and Microphysics. *J. Atmos. Sci.,* **62**, 4127–4150.

Tessendorf, S. A., K. C. Wiens, S. A. Rutledge, 2007: Radar and Lightning Observations of the 3 June 2000 Electrically Inverted Storm from STEPS. *Mon. Wea. Rev.*, **135**, 3665–3681.

Thomas, R., P. Krehbiel, W. Rison, J. Harlin, T. Hamlin, N. Campbell, 2003: The LMA flash algorithm. *Proc. 12th Int. Conf. on Atmospheric Electricity*, Versailles, France, International Commission on Atmospheric Electricity, 655-656.

Wiens, K. C., 2005: Kinematic, microphysical, and electrical structure and evolution of thunderstorms during the Severe Thunderstorm Electrification and Precipitation Study (STEPS). Ph.D. thesis, Colorado State University, Fort Collins, CO, 295 pp.

Wiens, K. C., S. A. Rutledge, S. A. Tessendorf, 2005: The 29 June 2000 Supercell Observed during STEPS. Part II: Lightning and Charge Structure. *J. Atmos. Sci.*, **62**, 4151–4177.

Williams, E. (1989): The Tripole Structure of Thunderstorms, *J. Geophys. Res.*, **94** D11, 13151-13167.

Williams, E. R., 2001: The electrification of severe storms. *Severe Convective Storms, Meteor. Monogr.*, No. 50, Amer. Meteor. Soc., 527–561.

Williams, E. R., V. Mushtak, D. Rosenfeld, S. Goodman, and D. Boccippio, 2005: Thermodynamic conditions favorable to superlative thunderstorm updraft, mixed phase microphysics and lightning flash rate. *Atmos. Res.*, **76**, 288–306.

Zajac, Bard A., Steven A. Rutledge, 2001: Cloud-to-Ground Lightning Activity in the Contiguous United States from 1995 to 1999. *Mon. Wea. Rev.*, **129**, 999–1019.